

University of Nevada, Reno

**CFD Simulations of an Air-Conditioned Radiological Materials Staging Room:  
Comparison Between COMSOL and ANSYS Codes**

A thesis submitted in partial fulfillment of the  
requirements for the degree of Master of Science in  
Mechanical Engineering

by

Frank Pulciano

Dr. Mustafa Hadj-Nacer/Thesis Advisor

December 2023



THE GRADUATE SCHOOL

We recommend that the thesis prepared  
under our supervision by

**Frank Pulciano**

Entitled

**CFD Simulations of an Air-Conditioned Radiological Materials Staging Room:  
Comparison Between COMSOL and ANSYS Codes**

be accepted in partial fulfillment of the requirements  
for the degree of

MASTER OF SCIENCE

Mustafa Hadj-Nacer, Ph. D., Advisor

Miles Greiner, Ph. D., Co-advisor

Aditiya Nair, Ph. D., Committee Member

Nicholas Tsoulfanidis, Ph. D., Committee Member

Markus Kemmelmeier, Ph.D., Dean, Graduate School

December 2023

# Abstract

---

Heat-generating radiological material packages, such as the 9975 package and other packages, are stored in facilities managed by the National Nuclear Security Administration (NNSA). These packages must be stored in a ventilated facility to prevent the packages, internal components, and outer surfaces from reaching prescribed limits. The objective of this work is to conduct steady-state computational fluid dynamics (CFD) simulations of a potential ventilated radiological-material-package staging facility to assess the surface temperatures of the packages using two CFD codes: ANSYS/Fluent finite volume and COMSOL finite element codes. The simulated facility contains 640 heat-generating 9975 packages, arranged in four rows and eight levels, equipped with a ventilation system and lighting. The outer walls of the facility are assumed to be completely insulated. The packages are modeled as Celotex insulation, each of them generating 19 W of heat. Due to the computational demands of COMSOL, the simulations excluded the modeling of natural convection and the shelving structure supporting the packages in both ANSYS and COMSOL simulations. For both CFD codes, three numerical meshes are generated and mesh sensitivities are conducted to determine the optimal meshes. The package maximum temperatures obtained using the optimal mesh for each code are compared and the differences are analyzed. The results show that the temperatures and flows in the staging facility vary depending on the CFD code used. ANSYS/Fluent predicts maximum package surface temperatures that are on average 5°C higher than COMSOL. Also, ANSYS/Fluent predicts the location of the hottest package to be near the back of the facility, while COMSOL predicts it toward the front. Additional simulations using both codes, isolating

conduction, convection, and radiation heat transfers have been conducted. The results showed that the two codes predict the same package surface temperatures when only conduction heat transfer is considered. However, discrepancies emerged when convection and radiation were included.

# Acknowledgment

---

I would like to express my deepest gratitude to Professor Mustafa Hadj-Nacer and Dr. Miles Greiner. Their invaluable guidance, unwavering support, and insightful feedback have played a pivotal role in shaping my research. I am truly fortunate to have had the privilege of working under their mentorship, and I appreciate the time and expertise they generously shared throughout this academic journey.

I would also like to give my heart felt appreciation to Dr. Nicholas Tsoulfanidis and Dr. Aditiya Nair, esteemed members of my thesis committee. Who together have helped me have a greater understanding of my research field and encouraged me to challenge myself while at my time at the University.

Special thanks to Alex, Aman, Antonio, Armin, Ashish, Brandon, Harrison, Iffat, Jamie, Kellen, Lily, Lucio, Mehrab, Merbin, Megan, Milad, Milad, Raven, Soumya, Subin, Teddy, and Thulani. All of your collective expertise, guidance, and support have been invaluable, shaping the trajectory of my life forever.

This work represents a collaborative effort between the Nevada National Security Sites, the University of Nevada, Reno, and the guidance of Dr. Mustafa Hadj-Nacer and Dr. Miles Greiner. Their collective contributions have significantly enhanced the quality and scope of the findings.

# Table of Contents

---

Abstract .....	i
Acknowledgment .....	iii
Table of Contents .....	iv
Nomenclature .....	ix
List of Tables .....	vi
List of Figures .....	vi
1. Introduction .....	1
2. Model Development .....	3
3. Mesh Refinement.....	6
3.1. COMSOL Meshes .....	7
3.2. ANSYS Meshes.....	8
4. Boundary Conditions and Numerical Approaches .....	10
4.1. Boundary Conditions.....	10
4.2. Numerical Approaches.....	11
5. Results .....	12
5.1. COMSOL Mesh Sensitivity Analysis .....	12
5.2. ANSYS Mesh Sensitivity Results .....	17

5.3. Comparison and Discussions .....	20
Conclusions.....	27
Acknowledgment .....	28
References.....	28

# List of Tables

---

Table 1: Number of solid and fluid elements and quality for the COMSOL meshes.....	8
Table 2: Number of solid and fluid elements and quality for the ANSYS meshes.....	10
Table 3: COMSOL steady state simulation results for all meshes.....	14
Table 4: ANSYS steady state simulation results for all meshes .....	18



# List of Figures

---

Figure 1: Three-dimensional model of a hypothetical staging facility for radiological packages .....	5
Figure 2: Schematic of the modeled staging facility with dimensions in meters. (a) $xz$ plane view and (b) $yz$ plane view .....	6
Figure 3: Meshes generated for the COMSOL model. The top images show the mesh elements on the packages' outer surfaces and the lower images show the mesh elements in the $yz$ -plane passing through the center of packages for (a) 2.8 M, (b) 5.1 M and (c) 10 M element meshes .....	7
Figure 4: Meshes generated for the ANSYS model. The top figures show the mesh elements on the packages' outer surfaces and the lower figures show the mesh elements in the $yz$ -plane passing through the center of packages for (a) 14.6 M, (b) 21.6 M and (c) 33.7 M element meshes.....	9
Figure 5: Temperature differences $\Delta T_{max}$ , $\Delta T_{out}$ , and $\Delta T_{out,EB}$ as function of iterations for the COMSOL meshes.....	14
Figure 6: Package-to-package maximum surface temperature comparison between meshes. a) $C_{3M}$ vs. $C_{10M}$ b) $C_{5M}$ vs. $C_{10M}$ .....	16
Figure 7: Temperature differences $\Delta T_{max}$ , $\Delta T_{out}$ , and $\Delta T_{out,EB}$ as function of iterations for the ANSYS/Fluent meshes .....	18
Figure 8: Package-to-package maximum surface temperature comparison between meshes. a) $A_{15M}$ vs $A_{34M}$ b) $A_{22M}$ vs $A_{34M}$ .....	19

Figure 9: Isometric package surface temperature contours for a) COMSOL model and b) ANSYS model.....	21
Figure 10: Air temperature and velocity vectors midway between Rows 2 and 3 at plane $x = 4.572$ m for a) COMSOL model $C_{5M}$ and b) ANSYS model $A_{22M}$ .....	22
Figure 11: Package-to-package maximum surface temperature comparison between COMSOL and ANSYS models.....	24
Figure 12: Package-to-package maximum surface temperature comparison between COMSOL and ANSYS models for a) three combinations and b) one combination of heat transfer mechanisms.....	25

# Nomenclature

---

$A$	ANSYS model
$C$	COMSOL model
$\dot{m}$	Mass flow rate
$\Delta P$	Pressure difference
$\Delta T_{avg}$	Difference between the average drum and inlet temperatures
$\Delta T_{max}$	Difference between maximum drum and inlet temperatures
$\Delta T_{out}$	Difference between outlet and inlet temperatures

## Subscripts

3M	2.76 million elements
5M	5.08 million elements
10M	9.95 million elements
15M	15 million elements
22M	22 million elements
34M	34 million elements

## 1. Introduction

Heat-generating radiological materials are stored in a variety of packages, like the 9975-package, by the Department of Energy (DOE). The 9975-package is a Type B, drum-shaped package that offers secure and legally compliant packaging for shipments of solid fissile and other radiological materials. It consists of a dual containment vessel made from 304L stainless steel, sealed with thick stainless-steel plugs and fluorocarbon elastomer O-rings. These vessels are encased in a lead shield and Celotex insulations, all placed within a stainless-steel drum [1]. The 9975 package was engineered to withstand thermal and structural loads for Normal Conditions of Transport (NCT) and Hypothetical Accident Conditions (HAC) to prevent the release of radiological materials into the environment and protect workers from harmful radiological effects. [1, 2]. The specific performance requirements for these packages are to (a) withstand structural loads under NCT and HAC, (b) maintain double containment under both NCT and HAC, (c) protect the containment vessels and lead shielding body from excessive heat in a regulatory fire event, and (d) provide impact protection in regulatory drop and puncture events to prevent mechanical damage to the containment vessels [2]. The regulatory requirements for all radiological packages that are designed and maintained for transport per the Code of Federal Regulations are to maintain accessible surfaces (outer surfaces) of packages below a temperature of 50°C in a “nonexclusive use” shipment, or 85°C in an “exclusive use” shipment [2]. “Exclusive use” means a single shipper transports the material and all initial, intermediate, and final loading and unloading are carried out in accordance with the direction of the shipper or receiver.

The 9975 package and other packages are stored in facilities managed by the National Nuclear Security Administration (NNSA). The NNSA has a broad mandate to safely store, ship, and dispose of radiological materials [3]. In order for these materials to remain in safe conditions, they must be placed in an environmentally controlled storage facility equipped with radiation and thermal monitoring [4]. The storage configuration must be accessible to meet programmatic needs and provide adequate cooling through forced convection, keeping package components, including outer surfaces, below prescribed temperature limits [1]. NNSA facilities typically store these packages on the floor. However, there is a growing interest in developing new types of staging facilities that can increase capacity, safety, and practicality [5]. The NNSA is currently exploring the use of steel racks for package storage. This new arrangement aims to facilitate easier retrieval of packages, reduce their temperature, and enhance worker safety [5].

Computational Fluid Dynamics (CFD) are used in food, building, and other industries to predict the performance of Heating, Ventilation, and Air Conditioning (HVAC) systems in maintaining facilities within prescribed temperature margins [6,7]. However, few works have considered the investigation of HVAC systems within the context of a staging facility for radiological packages. The only notable works that have been performed for a staging facility with radiological material packages are with heated boxes placed on racks [8, 9]. In these studies, a computational model for a radiological material staging building was created with adiabatic walls, heat-generating lights, and a large-scale rack system. For simplification, four packages were modeled as a single rectangular box-package generating heat equivalent to four 9975-type packages ( $4 \times 19\text{W}$ ). The facility included an HVAC system that provided cooling air into and out of the facility. A comparison was made

between two numerical solvers, Star CCM+ and ANSYS Fluent, and it was determined that both models were able to predict a similar location of the hottest box in the facility. Also, the models predicted the average surface temperature of the boxes within  $\pm 1^\circ\text{C}$ . A complete comparison between the two solvers was unable to be performed due to the unknown conditions of the models created in STAR CCM+. Furthermore, there are currently no experimental works in the open literature for radiological material staging facilities that can be used to validate the numerical models.

The objective of the present study is to conduct three-dimensional (3D) CFD simulations of a hypothetical ventilated radiological-material-package staging facility to determine the surface temperatures of the packages using ANSYS/Fluent and COMSOL codes. The simulated staging facility contains 640 9975-type packages arranged in four rows, eight levels, and five bays. The air supply and return ducts, as well as the lighting system, are included in the model. Each of the packages generated 19 W of heat and is modeled as Celotex insulation (the internal components of the packages are not modeled). This study aims to assess the difference between ANSYS/Fluent, based on the finite volume method (FVM), and COMSOL, based on the finite element method, in predicting the package surface temperatures.

## **2. Model Development**

Figure 1 shows a 3D isometric view of a hypothetical staging facility model constructed in SolidWorks. The facility has a rectangular shape with two indentations running the length of the long walls. This facility can store up to 640 packages in four rows. Each row contains five bays, each bay contains eight levels, and on each level, there are 4 packages.

The rows are numbered from 1 to 4, starting from the lowest point and going towards the highest point on the  $x$ -axis. The bays are numbered from 1 to 5, corresponding to the order of the  $y$ -axis values. The levels are numbered from 1 to 8, ranging from the bottom to the top. The figure also illustrates the package position numbering system, wherein each package is assigned a unique identifier based on its placement in terms of rows, bays, levels, and position, denoted as {Row, Bay, Level, Position}. For instance, the package nearest to the reference frame (located in the front left side corner, See Fig. 1) is represented as {1111}, signifying its location in row 1, bay 1, level 1, and position 1. Conversely, the package farthest from the reference frame is identified as {4584}, reflecting its placement in row 4, bay 5, level 8, and position 4. For simplicity, and based on prior research from the author's group, the steel shelving supporting the packages is not included in the model. The previous study [9] indicated that excluding shelving resulted in a negligible package temperature deviation (within  $0.6^{\circ}\text{C}$ ) compared to simulations with shelving. Furthermore, the current resources available to the researchers are insufficient to incorporate the shelving in the COMSOL model (as it requires far more resources than ANSYS), necessitating the packages to be modeled as if floating.

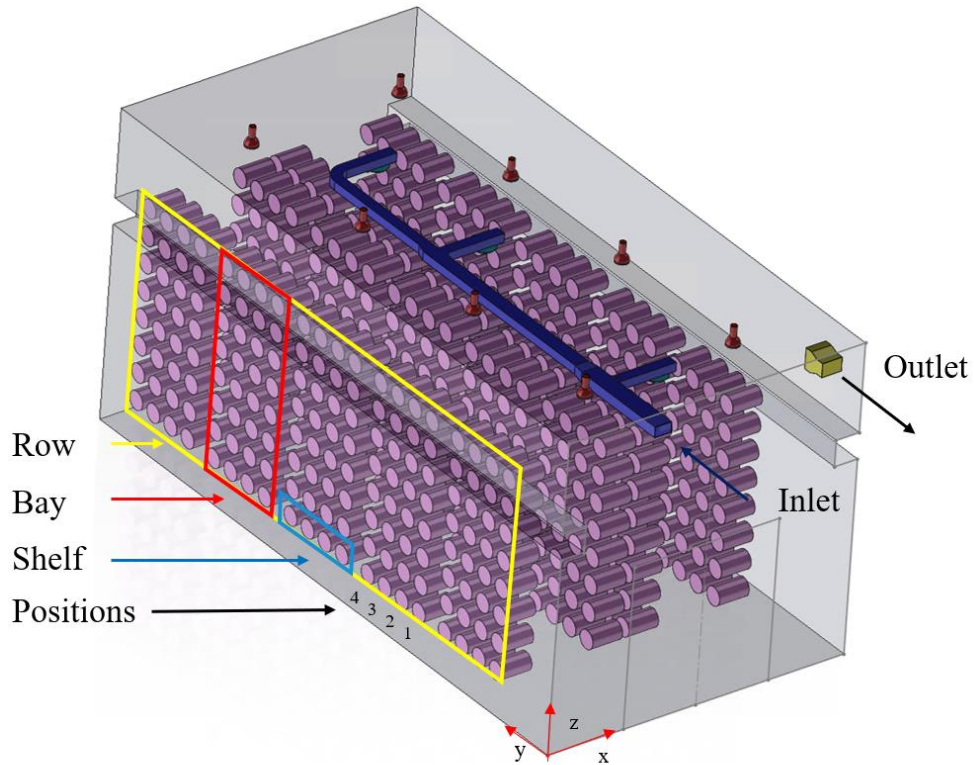


Figure 1: Three-dimensional model of a hypothetical staging facility for radiological packages.

Figure 1 also shows that near the ceiling of the facility, there are 8 lights, modeled as a half sphere (air with solid walls) topped with an aluminum cylinder, and supply and return ducts for the HVAC system. The supply duct comprises three plenums, directing airflow over a diffuser designed to expand the airflow toward the ceiling.

Figure 2 illustrates the dimensions of the proposed staging facility, which measures 18.44 m (60.5 ft) in length, 9.14 m (30 ft) in width, and 8.99 m (29.5 ft) in height. The two indentations along the length of the longer walls are at a height of 5.64 m from the ground, each measuring 0.71 m in width and 0.76 m in height. Each of the 640 packages measures 0.5334 m (21 in.) in diameter and 0.9144 m (36 in.) in length. Spatial arrangements within



the facility include a 0.20 m gap between the central rows, 1.88 m between the central rows and the side rows, and 0.76 m between the side rows and the facility side walls. The center-to-center distance between adjacent packages in different bays is 1.07 m, while that distance within the same bay is 0.70 m. Vertically, superposed packages are spaced by a 0.26 m gap, and the lowest package level is 0.26 m elevated from the floor. The distance from the door wall to the center of the first package along the  $x$ -direction is 3.20 m, and the distance from the back wall to the nearest package center in the same direction is 0.44 m.

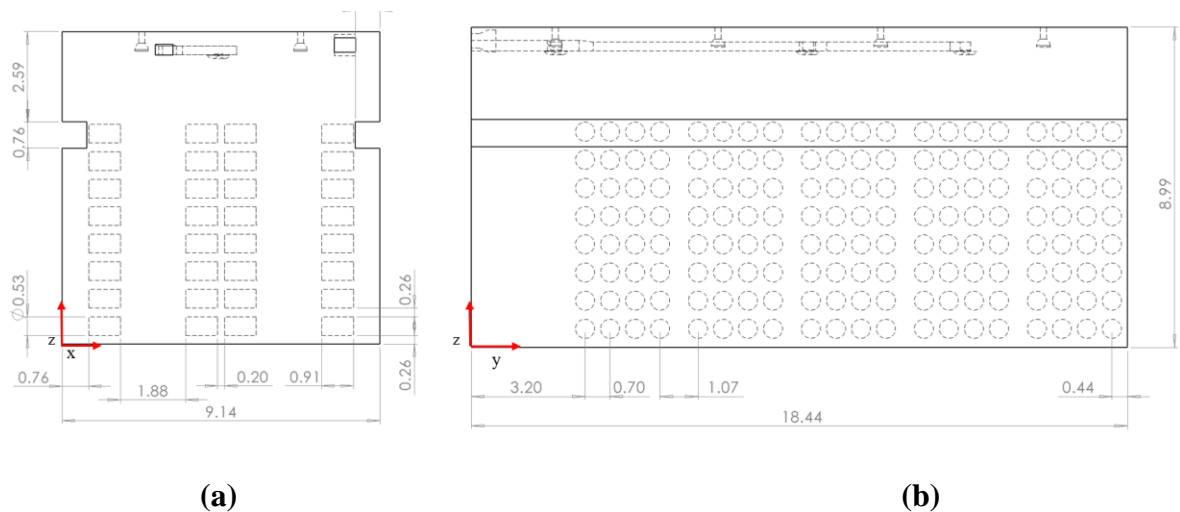


Figure 2: Schematic of the modeled staging facility with dimensions in meters. (a)  $xz$  plane view and (b)  $yz$  plane view.

### 3. Mesh Refinement

For each of the CFD codes considered, three computational meshes were generated and a mesh sensitivity analysis was performed to determine the optimal mesh. Details of the generated meshes and their respective qualities are discussed in this section, while the results of the mesh sensitivity analyses are presented in the Result Section.

### 3.1. COMSOL Meshes

Figure 3 shows the three tetrahedral element meshes generated in COMSOL for the purpose of conducting a mesh sensitivity analysis. These meshes are named according to the number of elements they contain, *i.e.*, 2.8 million ( $C_{3M}$ ), 5.1 million ( $C_{5M}$ ), and 10.0 million ( $C_{10M}$ ), with the letter C denotes COMSOL. Each mesh incorporates five inflation layers at the air-solid interfaces to better represent the flow and thermal boundary layers. It can be seen that as the mesh element count increases, a more precise representation of the cylindrical package geometry is obtained, suggesting a more accurate volume approximation with the finest mesh ( $C_{10M}$ ).

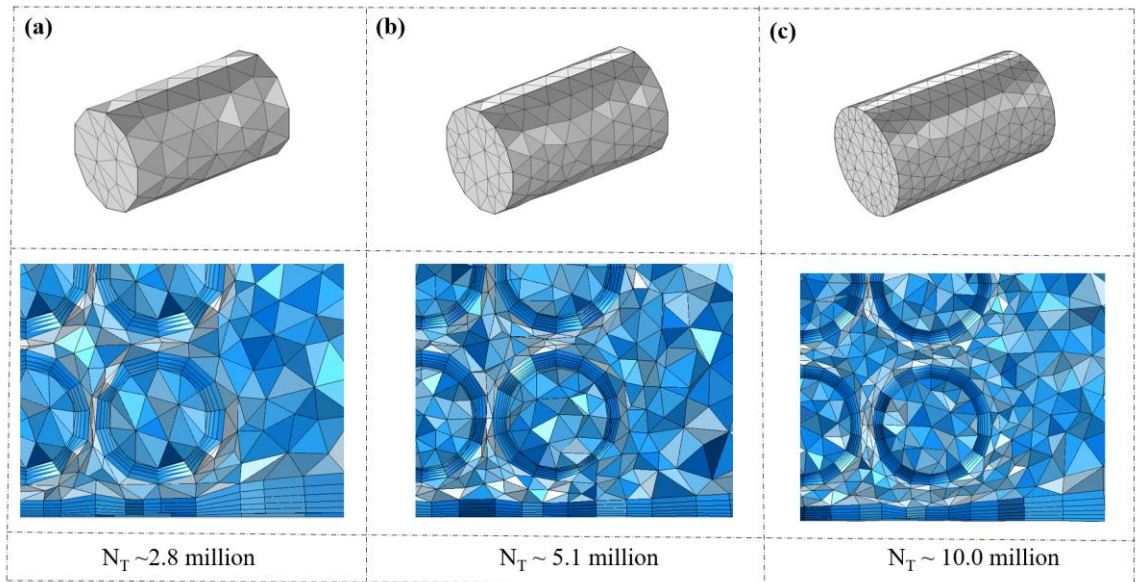


Figure 3: Meshes generated for the COMSOL model. The top images show the mesh elements on the packages' outer surfaces and the lower images show the mesh elements in the  $yz$ -plane passing through the center of packages for (a) 2.8 M, (b) 5.1 M and (c) 10 M element meshes.

Table 1 shows the number of fluid elements ( $N_F$ ), solid elements ( $N_S$ ), and total elements ( $N_T$ ) for each of the three COMSOL meshes. Solid elements constitute

approximately 9% to 13% of the total, with the remainder being fluid elements. The quality of the mesh elements assessed in terms of average skewness and orthogonal quality is also provided in Table 1. These metrics indicate the quality of the average element in the meshes. Maintaining high orthogonality and a low skewness of the mesh elements is imperative for grid quality, contributing to the accuracy and stability of the numerical solution in CFD simulations. For all three meshes, the average skewness is approximately 0.62, significantly below one, and the average orthogonal quality is 0.75, significantly above zero. The general rule of thumb is that the skewness should be less than 0.85 and the minimum orthogonal quality should be more than 0.1 to avoid instability in the simulations.

Table 1: Number of solid and fluid elements and quality for the COMSOL meshes.

	$C_{3M}$	$C_{5M}$	$C_{10M}$
$N_F$	2,510,679	4,524,949	8,678,712
$N_S$	257,805	562,764	1,271,260
$N_T$	2,768,484	5,087,713	9,949,972
<b>Average Skewness</b>	0.60	0.62	0.64
<b>Average Orthogonality</b>	0.75	0.75	0.75

### 3.2. ANSYS Meshes

Figure 4 illustrates the polyhedral cell meshes generated in ANSYS, named  $A_{15M}$ ,  $A_{22M}$ , and  $A_{34M}$ , comprising approximately 14.6 million, 21.6 million, and 33.6 million cells, respectively. The prefix “A” letter denotes ANSYS. Initially, tetrahedral cells were generated and subsequently converted into polyhedral cells to lower the cell count and enhance the mesh quality. One may notice that the coarsest ANSYS mesh,  $A_{15M}$ , has a

higher cell count than the finest COMSOL, with 10 million elements. This difference arises from ANSYS's utilization of the FVM which inherently requires a larger number of mesh cells. FVM uses a control volume approach to discretize the domain, where the conservation equations are solved at the center of the cells (control volumes).

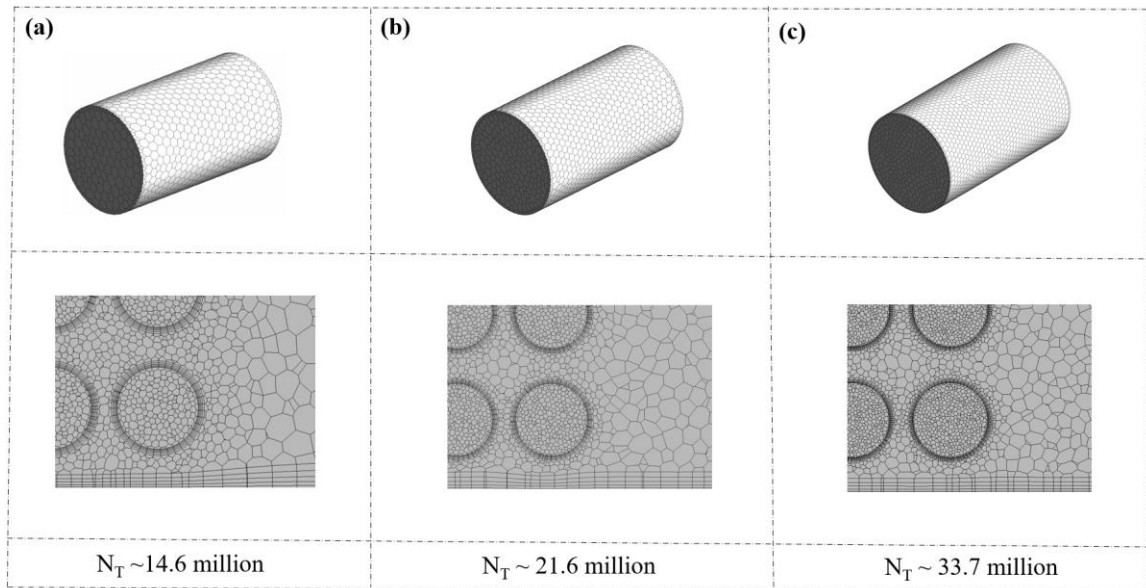


Figure 4: Meshes generated for the ANSYS model. The top images show the mesh elements on the packages outer surfaces and the lower images show the mesh elements in the  $yz$ -plane passing through the center of packages for (a) 14.6 M, (b) 21.6 M and (c) 33.7 M element meshes.

Table 2 provides the number of cells ( $N_F$ ,  $N_S$ ,  $N_T$ ) for each ANSYS mesh. The solid cells represent 24% to 34% of the total, which is a higher ratio compared to the COMSOL meshes. For all three ANSYS meshes, the average skewness is in the range of 0.068 to 0.074, below the threshold of 0.85, and the average orthogonal quality ranges from 0.922 to 0.929, above the recommended minimum of 0.10. These metrics indicate high-quality meshes, likely to yield stable and accurate simulation results.

Table 2: Number of solid and fluid elements and quality for the ANSYS meshes.

	$A_{15M}$	$A_{22M}$	$A_{34M}$
<b>N<sub>S</sub></b>	3,568,445	6,281,625	11,407,678
<b>N<sub>F</sub></b>	11,065,853	15,348,120	22,319,434
<b>N<sub>T</sub></b>	14,634,298	21,629,745	33,727,112
<b>Average Skewness</b>	0.074	0.072	0.068
<b>Average Orthogonality</b>	0.922	0.925	0.929

#### 4. Boundary Conditions and Numerical Approaches

Steady-state simulations that include conduction, radiation, and forced convection heat transfer, are conducted in both COMSOL and ANSYS/Fluent. Natural convection was not modeled because it requires considerable computational resources, particularly in COMSOL, beyond the available resources. For radiation heat transfer, the surface-to-surface (S2S) model in COMSOL and the Discrete Ordinate (DO) model in ANSYS/Fluent were utilized. A separate study (not presented here) comparing the S2S model with the DO model in ANSYS/Fluent indicated negligible differences. The  $k-\varepsilon$  turbulence model was employed to account for flow turbulence in the facility with automatic wall treatment used in COMSOL and the Standard Wall Function in ANSYS/Fluent.

##### 4.1. Boundary Conditions

The facility's 640 packages generate 19 W of heat each and are modeled as Celotex insulation [1], neglecting their internal components. Additionally, the eight facility lights generate 100W of heat each, totaling 12,960 W of heat generation within the facility. The HVAC system supplies 0.78906 kg/s of air at a temperature of 17.78°C (64°F) through three diffusers and allows air to freely return through one return duct. The outer surfaces

of the packages radiate to the surrounding with an emissivity of 0.21 and the outer walls of the facility are assumed to be adiabatic (insulated) with an internal emissivity value of 1. Constant thermal properties are used for both the fluid and solid regions. The facility's internal pressure is set initially at 1 atm, with a zero-gauge pressure maintained at the outlet.

## **4.2. Numerical Approaches**

COMSOL and ANSYS/Fluent codes employ different numerical approaches, FEM and FVM, to solve the nonlinear partial differential equations (PDEs) of continuity, momentum, and energy conservation, respectively. Both methods use numerical approximations to solve the PDEs, however, they differ in their modeling approaches. To discretize the flow domain, FEM subdivides it into a finite number of small, interconnected elements. The connections between the elements are called nodes. The weak form of the governing equations is then applied to the discretized domain. This involves multiplying the equations by test functions and integrating over the entire domain, transforming the PDEs into integral equations. Compared to the equation's original strong form, this weak form features derivatives that are simpler and of lower order, suitable for numerical solution [11].

The FVM approach on the other hand is more intuitive for fluid and thermal applications. In FVM, the domain is divided into small control volumes (cells), and the conservation equations are integrated over the volume of each cell. By assuming that the flux varies linearly at the entry and exit of the cells, the fluxes at the cell boundaries (faces) are approximated, transforming the integral equations into a set of algebraic equations. These equations are interconnected, with the flux exiting one cell becoming the influx for

the adjacent cell. Solving these equations simultaneously, typically using matrix techniques, yields the flow and thermal fields throughout the domain [12].

Both FEM and FVM have distinct strengths and limitations in modeling flow and heat transfer problems. In general, FEM is advantageous for its flexibility in handling complex geometries and boundary conditions, offering high accuracy in targeted regions. However, this method is computationally intensive. On the other hand, FVM better conserves fundamental quantities like mass, momentum, and energy, making it ideal for fluid flow and heat transfer simulations. It is intuitive and straightforward, performing well even with coarser meshes, but faces challenges with complex geometries and may not achieve the localized accuracy of FEM. The choice between these methodologies typically depends on the specific requirements of the CFD problem, including the complexity of the geometry, the nature of the flow, and the computational resources available.

## 5. Results

In this section, the results of the mesh sensitivity analysis for each of the COMSOL and ANSYS/Fluent codes are first presented to determine the optimal meshes and the mesh independence. Then, a comparison between the results from the two codes is discussed.

### 5.1. COMSOL Mesh Sensitivity Analysis

Figure 5 and Table 3 present the results of the mesh sensitivity analysis for the three COMSOL meshes. Figure 5 shows the maximum package surface temperature differences,  $\Delta T_{max}$ , and the average outlet temperature difference,  $\Delta T_{out}$ , as a function of the number of iterations.  $\Delta T_{max}$  is defined as the maximum package surface temperature minus the

inlet temperature,  $T_{in}$ , and  $\Delta T_{out}$  is defined as the average outlet temperature minus  $T_{in}$ .

The energy balance outlet temperature difference,  $\Delta T_{out,EB}$ , calculated as

$$\Delta T_{out,EB} = \frac{\dot{Q}_{total}}{\dot{m}_{out}c_p}, \quad (1)$$

where  $\dot{Q}_{total}$  is the total heat generation rate and  $c_p$  is the specific heat of air at constant pressure, is shown as a solid horizontal line. This figure shows that both temperature differences reach constant values at around 300 iterations. The average outlet temperature difference  $\Delta T_{out}$  obtained from the different meshes is nearly the same and converges to the energy balance outlet value  $\Delta T_{out,EB}$ . This means that energy is accurately conserved in all meshes. The obtained maximum temperature differences,  $\Delta T_{max}$ , is higher for the coarse mesh,  $C_{3M}$ , compared to the other two meshes, which exhibit nearly the same values. The steady-state values of the temperature differences are listed in Table 3.

Table 3 also shows the steady state values of the pressure difference between the inlet and outlet of the facility,  $\Delta P$ , and the outlet mass flow rate,  $\dot{m}_{out}$ , in addition to  $\Delta T_{max}$ ,  $\Delta T_{out}$ ,  $\Delta T_{out,EB}$ , and  $\Delta T_{avg}$ , which is defined as the packages' average surface temperature minus  $T_{in}$ . These values were averaged over the last 100 iterations. Both the pressure difference and outlet mass flow rates predicted by the three meshes are the same. The outlet mass flow rate is identical to the inlet prescribed value, which means that the mass within the system is conserved.  $\Delta T_{avg}$  for the coarse and fine mesh are similar but smaller than the coarse mesh.

The total number of iterations to achieve the required energy and flow residuals of  $10^{-6}$  and the computational time are shown in Table 3 for each mesh. A workstation with 64 cores and 512 GB of RAM was used for the simulations. The total number of iterations



is the sum of the iterations required for the flow and thermal simulations, as COMSOL was run in segregated mode to reduce the computational resources. The total number of iterations for all the meshes is nearly the same. Considering the small difference in the total number of iterations, one may notice that the total computational time increases almost linearly with the number of mesh elements.

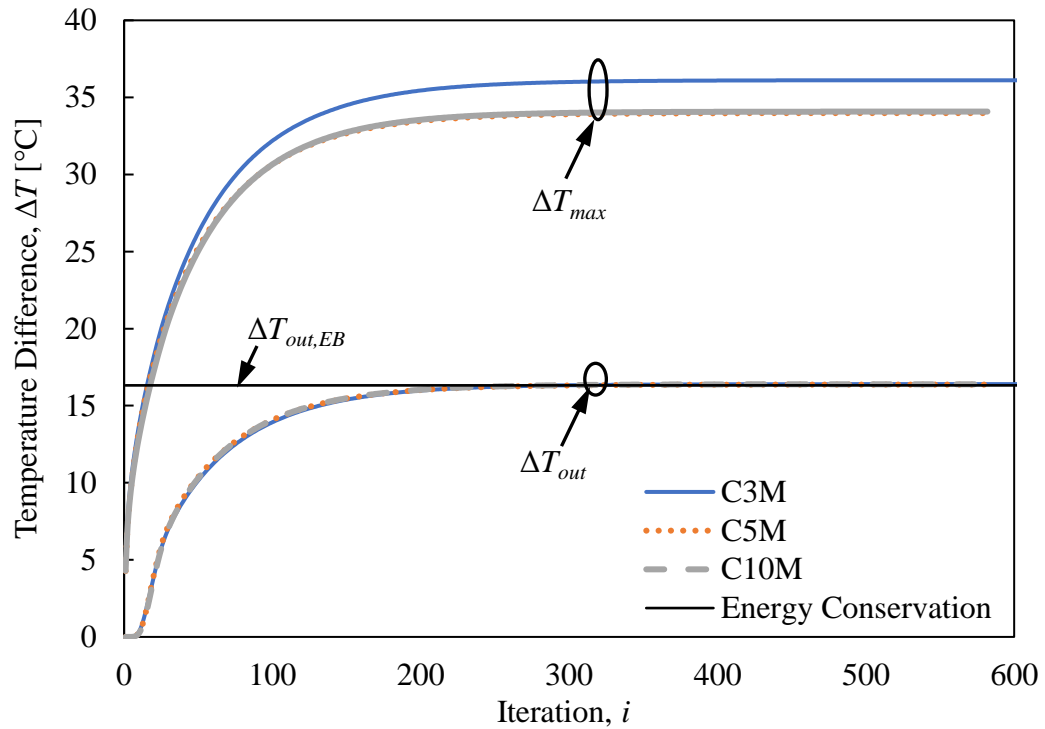


Figure 5: Temperature differences  $\Delta T_{max}$ ,  $\Delta T_{out}$ , and  $\Delta T_{out,EB}$  as function of iterations for the COMSOL meshes.

Table 3: COMSOL steady state simulation results for all meshes.

Mesh	$\Delta P$ [Pa]	$\dot{m}$ [kg/s]	$\Delta T_{out}$ [°C]	$\Delta T_{out,EB}$ [°C]	$\Delta T_{max}$ [°C]	$\Delta T_{avg}$ [°C]	N° of Iterations	Computational time
$C_{3M}$	50.0	0.7891	16.40	16.32	36.11	25.04	754	17 hrs 42 min
$C_{5M}$	50.0	0.7891	16.37		33.98	23.74	721	30 hrs 21 min
$C_{10M}$	50.0	0.7891	16.39		34.08	23.71	820	66 hrs 16 min

Figures 6a and 6b present a package-to-package maximum surface temperature comparison between the COMSOL meshes. Figure 6a compares the coarse  $C_{3M}$  mesh to fine  $C_{10M}$  mesh, and Fig. 6b compares the medium  $C_{5M}$  mesh to the fine  $C_{10M}$  mesh. The diagonal solid line represents the case where the lower element count meshes reproduce the data of the fine mesh perfectly. The dashed line represents the linear fit line of the data with its equation shown in the figures. The two dashed-dotted lines are the 95% standard error of the estimate,  $S_{95\%}$ , of the data calculated as

$$S_{95\%} = 2 \sqrt{\frac{\sum (T_{max,Y} - [aT_{max,X} + b])^2}{n - 2}}, \quad (2)$$

where  $T_{max,Y}$  and  $T_{max,X}$  are the maximum package surface temperatures for the y-axis and x-axis meshes, respectively. Each mesh package location is plotted against the corresponding package location in the other mesh. This enables the assessment of the variance between two meshes.

Figure 6a shows that the coarse  $C_{3M}$  mesh systematically overpredicts the maximum surface package temperatures compared to the fine  $C_{10M}$  mesh in almost all packages. However, the medium  $C_{5M}$  mesh predicts the same maximum temperature as the fine  $C_{10M}$  mesh, within a 95% confidence interval of  $\pm 2.27^\circ\text{C}$ , See Fig. 6b. The spread of the temperature data may be due to different flow patterns within the facility for the different meshes. However, its effect on the results is not very significant, especially for the medium  $C_{5M}$  mesh. This result and those presented in Fig. 5 and Table 3 show that the coarse mesh  $C_{5M}$  is enough resolved to predict the same results as the fine mesh. This mesh will be used for subsequent comparisons with ANSYS/Fluent.

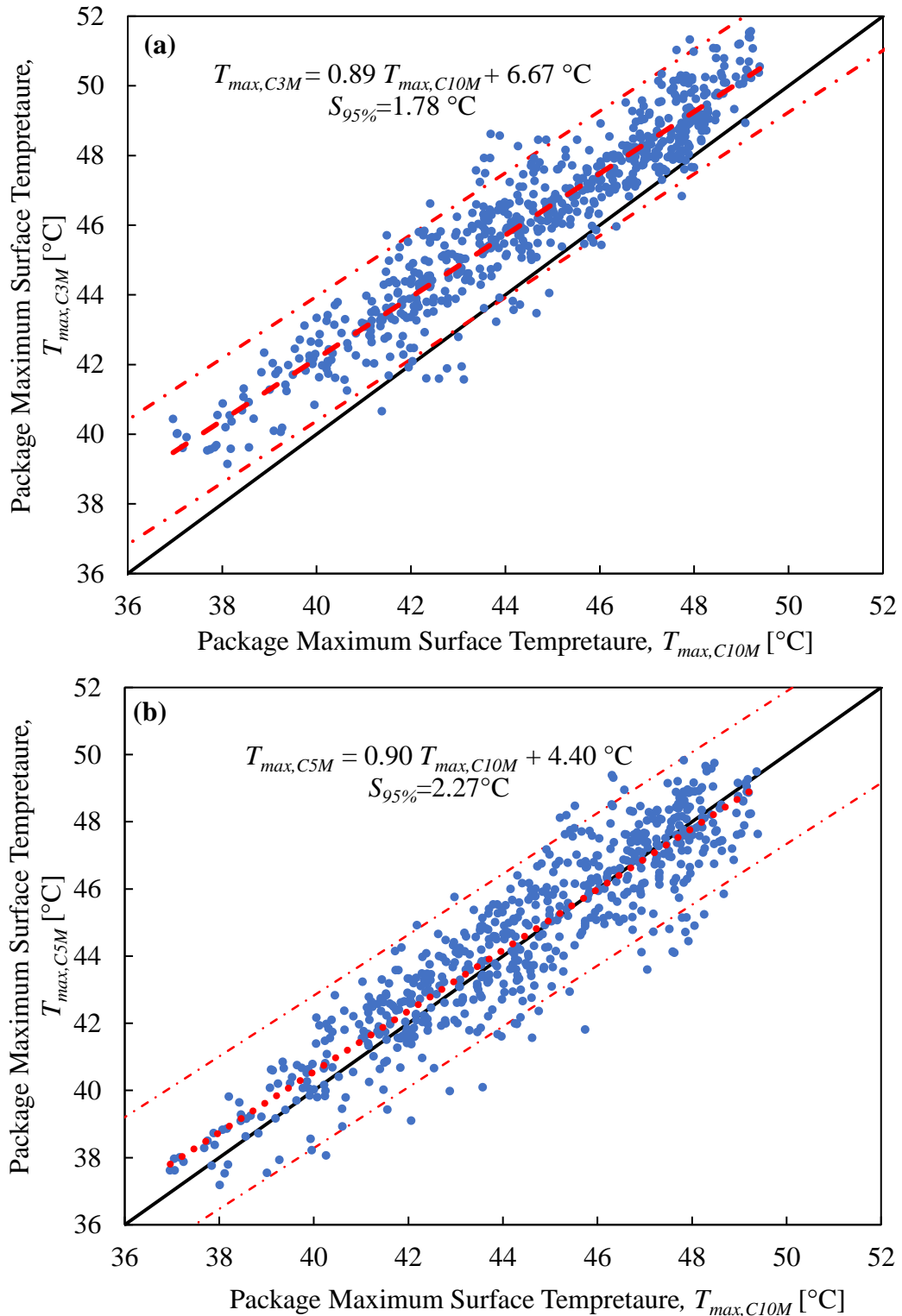


Figure 6: Package-to-package maximum surface temperature comparison between meshes. a)  $C_{3M}$  vs.  $C_{10M}$  b)  $C_{5M}$  vs.  $C_{10M}$ .

## 5.2. ANSYS Mesh Sensitivity Results

Figure 7 and Table 4 display the results of the mesh sensitivity for ANSYS/Fluent. Similar to Fig. 5, Fig. 7 shows the temperature differences  $\Delta T_{max}$ ,  $\Delta T_{out}$ , and  $\Delta T_{out,EB}$  as a function of iterations for the three ANSYS meshes  $A_{15M}$ ,  $A_{22M}$  and  $A_{34M}$ . All the three ANSYS meshes display an oscillatory behavior in the temperature differences. However, these oscillations are smaller for the average outlet temperature difference  $\Delta T_{out}$  compared to the maximum package surface temperature difference,  $\Delta T_{max}$ . Comparing  $\Delta T_{out}$  with  $\Delta T_{out,EB}$ , one can deduce that all three meshes accurately conserve energy. The oscillations of the maximum and average temperature differences for the coarse  $A_{15M}$  are lower than the coarse  $A_{22M}$  and fine  $A_{34M}$  meshes. After about 3000 iterations, a nearly repeating pattern is observed for all the temperature differences. By averaging the results over the last 2000 iterations, one can notice that the steady state values of  $\Delta T_{max}$  obtained for the medium and fine meshes are nearly the same, while the values for the coarse mesh are lower. The values of the steady-state temperature differences are presented in Table 4.

Table 4 also shows the pressure difference and the outlet mass flow rates for the three ANSYS meshes. The outlet mass flow rate remains consistent across all meshes, aligning with the specified inlet mass flow rate. However, the pressure difference between the inlet and outlet is similar for the two coarser meshes, but approximately 1.75 Pa higher for the finest mesh. This discrepancy is not well understood.

The computational time required to run the ANSYS meshes for 5000 iterations is shown in Table 4. The same workstation used in COMSOL simulations is used for ANSYS simulations. The results show that the computational time increases almost linearly with the number of mesh elements.

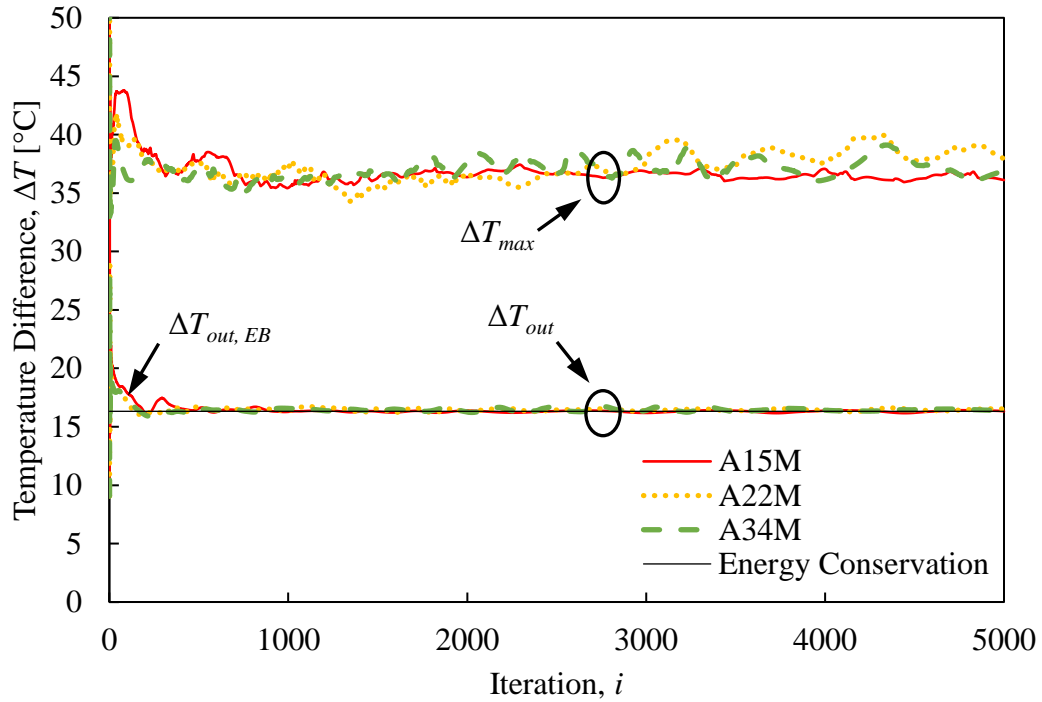


Figure 7: Temperature differences  $\Delta T_{max}$ ,  $\Delta T_{out}$ , and  $\Delta T_{out,EB}$  as function of iterations for the ANSYS/Fluent meshes.

Table 4: ANSYS steady state simulation results for all meshes.

Mesh	$\Delta P$ [Pa]	$\dot{m}$ [kg/s]	$\Delta T_{out}$ [°C]	$\Delta T_{out,EB}$ [°C]	$\Delta T_{max}$ [°C]	$\Delta T_{avg}$ [°C]	N° of Iterations	Computational time
$A_{15M}$	45.1	0.7891	16.29	16.32	36.09	26.18	5000	54 hrs 29 min
$A_{22M}$	45.4	0.7891	16.42		37.92	26.84	5000	131 hrs 17 min
$A_{34M}$	47.0	0.7891	16.42		36.72	27.14	5000	170 hrs 53 min

Figures 8a and 8b show package-to-package maximum surface temperature comparison between the  $A_{15M}$  and  $A_{34M}$  meshes, and  $A_{22M}$  and  $A_{34M}$  meshes, respectively. The solid, dashed, and dashed-dotted lines are the same lines defined in Figure 6. Most of the package maximum surface temperatures predicted by the coarse  $A_{15M}$  mesh are lower

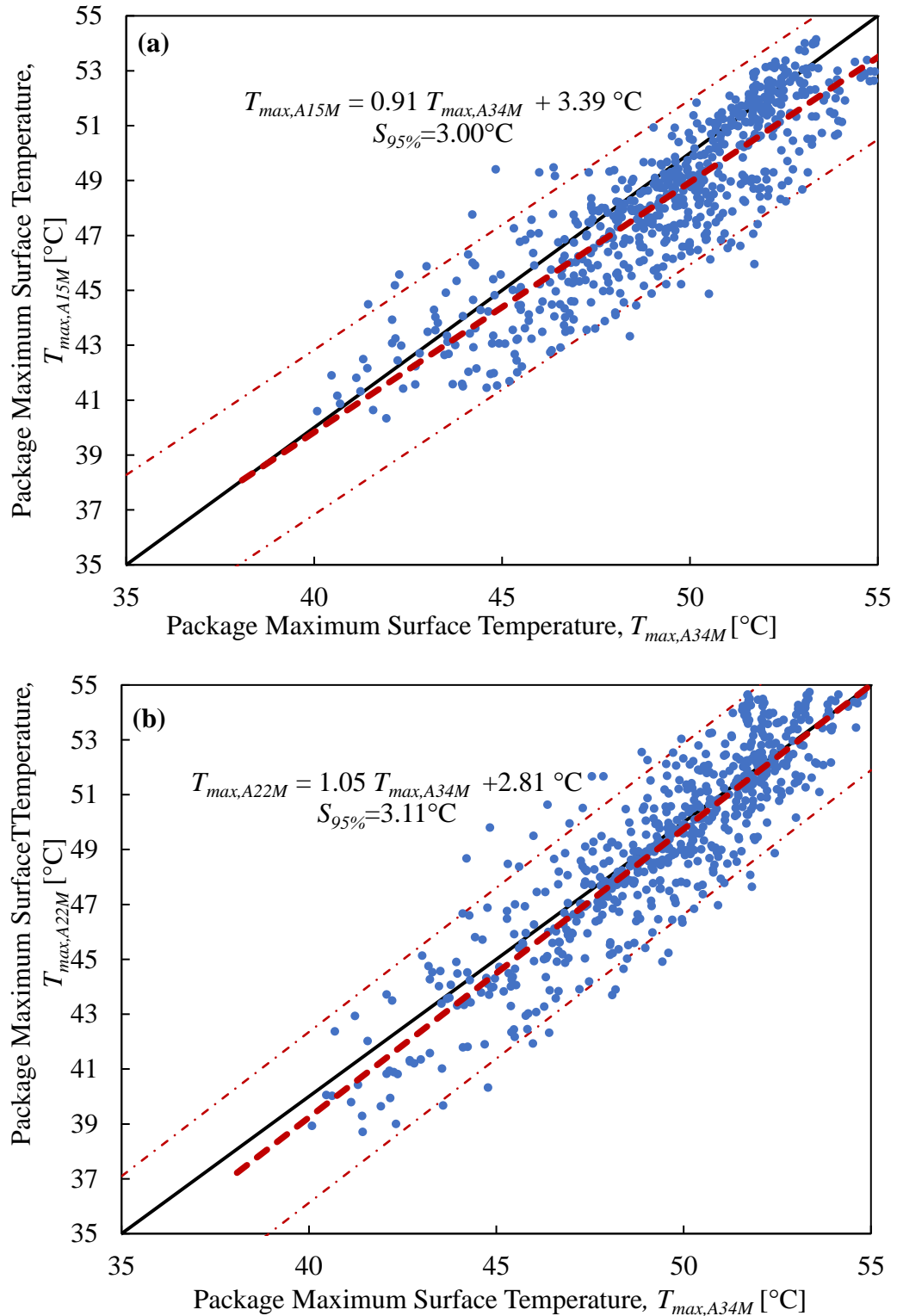


Figure 8: Package-to-package maximum surface temperature comparison between meshes. a)  $A_{15M}$  vs  $A_{34M}$  b)  $A_{22M}$  vs  $A_{34M}$ .

than fine  $A_{34M}$  mesh. However, the values predicted by the medium  $A_{22M}$  mesh are closer to the fine mesh, with a 95% confidence interval of  $3.11^{\circ}\text{C}$ . The small difference between the  $A_{22M}$  and  $A_{34M}$  mesh suggests that the medium mesh has a sufficient resolution to capture the flow and thermal behaviors within the storage facility. This mesh will be used for all subsequent comparisons with COMSOL.

### 5.3. Comparison and Discussions

The medium meshes of COMSOL ( $C_{5M}$ ) and ANSYS ( $A_{22M}$ ) are used to conduct the comparison between the two codes as they demonstrated mesh independence. Tables 3 and 4 show that the two models predict pressure differences within 5 Pa of each other, with COMSOL predicting the highest value. However, both models accurately conserve mass and energy, as shown in Sections 5.1 and 5.2. This table also shows that ANSYS predicts higher temperature difference  $\Delta T_{max}$  and  $\Delta T_{avg}$  by about  $3^{\circ}\text{C}$  to  $4^{\circ}\text{C}$ .

Figures 9a and 9b display a full isometric view of the temperature contours of the package surfaces for the COMSOL and ANSYS models, respectively. Both contours exhibit low temperatures at the packages close to the ceiling and higher temperatures at lower levels. The location of the coolest packages at the upper level is toward the back of the facility (high y-coordinate) in the COMSOL model and toward the front of the facility (low y-coordinate) in the ANSYS model. However, the location of the hottest packages in lower levels is toward the front of the facility in the COMSOL model and the back of the facility in the ANSYS model. This opposite behavior is due to the inverse flow direction in the COMSOL and ANSYS models.

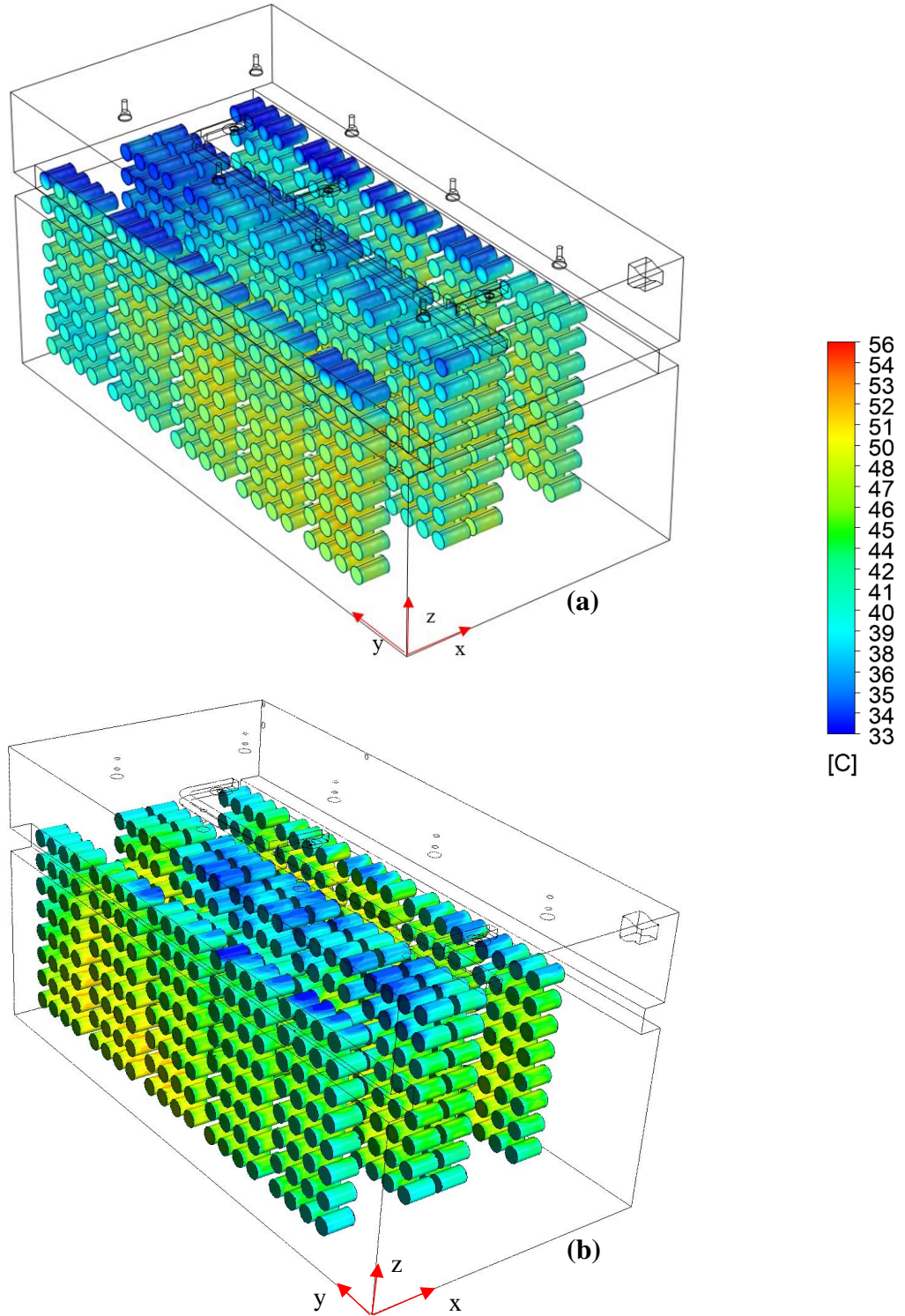


Figure 9: Isometric package surface temperature contours for a) COMSOL model and b) ANSYS model.



Figures 10a and 10b display the temperature contours with airflow velocity vectors in the midplane between Rows 2 and 3 (at  $x = 4.572$  m) for the COMSOL and ANSYS models, respectively. The velocity vectors shown are the tangential components of the air velocity in that plane.

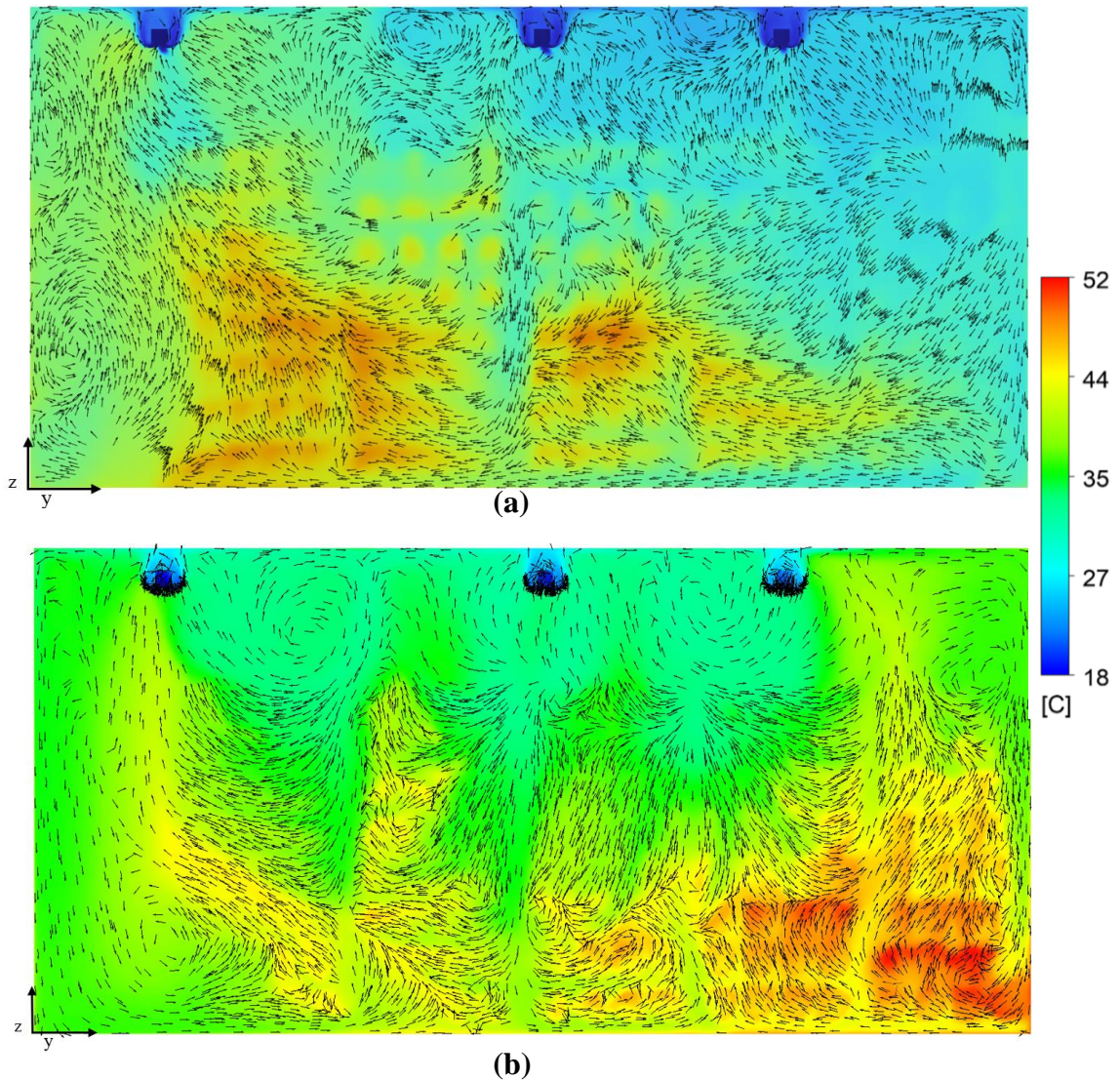


Figure 10: Air temperature and velocity vectors midway between Rows 2 and 3 at plane  $x = 4.572$  m for a) COMSOL model  $C_{5M}$  and b) ANSYS model  $A_{22M}$ .

Figure 10a shows that, for the COMSOL model, the airflow between the middle rows is predominately directed toward the front of the facility (negative y-direction) causing the packages in the back of the facility to be cooler than those in the front, where the highest temperatures occur. For the ANSYS model, Fig. 10b shows the opposite behavior, where the flow is mostly directed toward the back of the room (positive y-direction) causing the highest temperatures to concentrate in that region. Also, it can be noticed that the air near the front of the room (in the open region between the door and the first packages) is warmer in the COMSOL model than in the ANSYS model. This is again due to the opposite directions of the airflows.

Figure 11 displays the package-to-package surface temperature comparison between the COMSOL and ANSYS models. Most of the data is above the diagonal solid line, representing the case where the ANSYS results perfectly reproduce the COMSOL data. This figure shows that, overall, the ANSYS model overpredicts the package maximum temperatures compared to COMSOL by as much as 13°C. On average, ANSYS predicts a hotter maximum package surface temperature by about 4.4°C higher than COMSOL. The maximum package surface temperatures obtained from the COMSOL and ANSYS models are 49.83°C and 54.4°C, respectively. The ANSYS value is about 5°C above the temperature limit of 50°C set by the 10 CFR 7.43(g) [2]. The location of the hottest package in COMSOL is 2231 (2<sup>nd</sup> Row, 2<sup>nd</sup> Bay, 3<sup>rd</sup> level, and 1<sup>st</sup> position), while this location in ANSYS is 3533 (3<sup>rd</sup> Row, 5<sup>th</sup> Bay, 3<sup>rd</sup> level, and 3<sup>rd</sup> position). This shows there is a significant discrepancy between the COMSOL and ANSYS models in predicting the location of the hottest package within the staging facility.

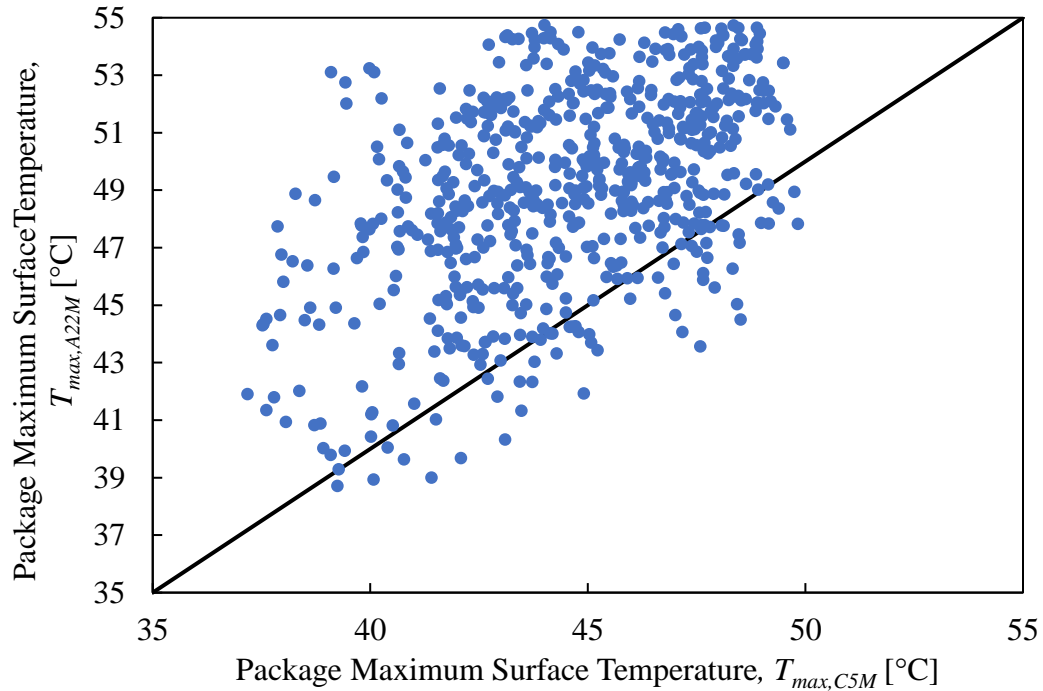


Figure 11: Package-to-package maximum surface temperature comparison between COMSOL and ANSYS models.

To understand the source of the discrepancy in the temperature results and maximum package location between the two codes, simulations were conducted where one mechanism of heat transfer was neglected at a time. Since the previous simulations were conducted using adiabatic facility outer walls, neglecting forced convection heat transfer (by closing the inlet and outlet) would result in an infinite temperature. Therefore, for the subsequent verification simulations, a constant facility outer wall temperature of  $17.78^{\circ}\text{C}$  was used.

Figure 12 shows the package-to-package maximum surface temperature comparison, between the COMSOL and ANSYS models for four different combinations of heat transfer mechanisms. Figure 12a shows three combinations a) all modes of heat transfer, b) conduction and radiation, and c) only radiation, while the “only conduction” case was plotted separately in Fig. 12b because of the large difference in scale.

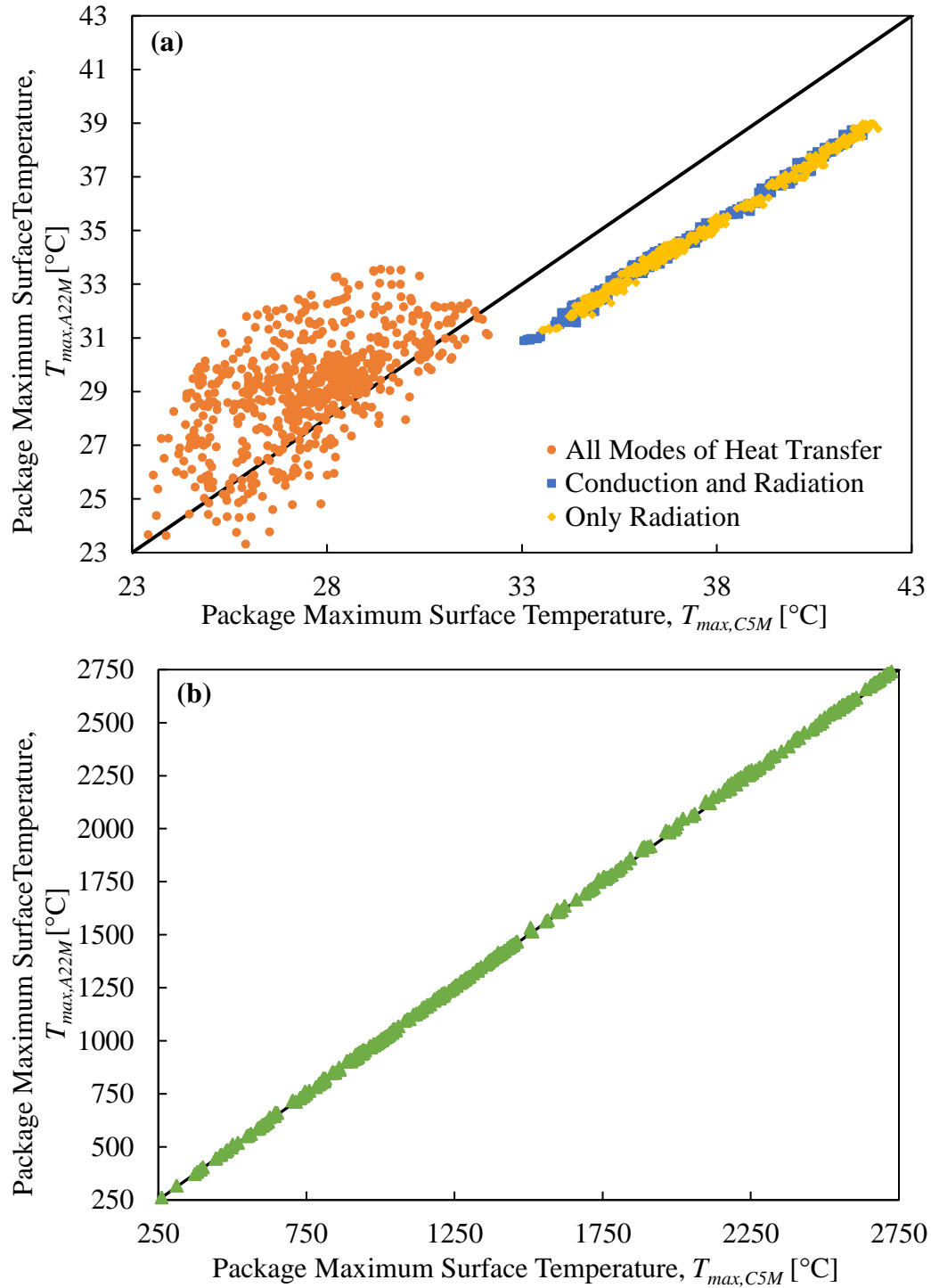


Figure 12: Package-to-package maximum surface temperature comparison between COMSOL and ANSYS models for a) three combinations and b) one combination of heat transfer mechanisms.

The maximum package surface temperatures obtained for the case with “All Modes of Heat Transfer” shown in Fig. 12a are significantly lower than those obtained in Fig. 11 due to the constant outer wall temperature of 17.78°C used in those simulations. However, the overall trend is similar, where the ANSYS model predicts higher temperatures than the COSMOL model. Neglecting forced convection heat transfer (“conduction and radiation” case) causes the temperature of the packages to significantly increase. An opposite trend is observed in this case, where the ANSYS temperatures became lower than the COMSOL values. Also, the obtained maximum package temperature data lies within a narrow range with nearly a constant difference between the models. These results indicate the two models (COMSOL and ANSYS) simulate the flow within the facility differently. This difference could be caused by the use of different wall treatments in the  $k-\varepsilon$  turbulence model. The constant difference between the two models, when forced convection is neglected, means that there is a systematic difference between the two models in simulating radiation and conduction heat transfer. Two more simulations were conducted where only radiation (Fig. 12a) and only conduction (Fig. 12b) heat transfer were accounted for. The results obtained from the “only radiation” case are very similar to the “conduction and radiation” case, with very small differences. This suggests that the systematic difference between the two models is caused by the way each code solves for radiation heat transfer and that the contribution of conduction heat transfer is negligible. This result is further confirmed in Fig. 12b. This figure shows that when only conduction heat transfer is considered, the maximum temperature of the packages becomes very high, suggesting that the contribution of conduction heat transfer is negligible compared to the other mode of

heat transfer. This figure also shows that data lies closely on the diagonal solid line, indicating that the two codes model conduction heat transfer similarly.

The above analysis showed that the two important mechanisms of heat transfer within the staging facility are forced convection and radiation heat transfer. However, the COMSOL and ANSYS codes solve both heat transfer mechanisms differently, which explains the significant difference between the models. It is hard to know the exact difference between the codes in modeling those heat transfer mechanisms because of the restricted access to their source codes.

## **Conclusions**

The NNSA is interested in developing efficient and safe methods to stage radiological material that meets the requirements of 10 CFR 830 [4]. In this study, a hypothetical staging facility is designed to stage a high-density configuration of heat-generating radiological material packages. Each of the 640 packages staged in this facility generates 19 W of heat. The facility has eight lights, generating a total of 800 W, and an HVAC system that supplies air through three diffusers at a temperature of 17.78°C. CFD simulations were conducted to predict the maximum outer surface temperatures of the packages using COMSOL and ANSYS codes. The outer walls of the facility are assumed to be adiabatic. A mesh sensitivity analysis was conducted to determine the optimal mesh for each code. The results of the comparison between the two codes showed a significant discrepancy in the maximum package surface temperatures. Specifically, ANSYS predicts higher package temperatures than COMSOL by as much as 13°C in a few locations. On average, ANSYS predicts the maximum package surface temperatures to be about 5°C higher than

COMSOL. Furthermore, the locations of the highest package temperatures predicted by the two codes are different, where ANSYS predicts them toward the back of the facility, while COMSOL predicts them toward the front. Additional simulations were conducted in both ANSYS and COMSOL to understand the source of the discrepancy between the codes. These simulations were conducted by neglecting the three mechanisms of heat transfer (conduction, forced convection, and radiation) one at a time. These simulations revealed that both codes model conduction heat transfer similarly but differ greatly in modeling radiation and forced convection heat transfers. Additionally, the results showed that radiation and forced convection are the most important heat transfer mechanisms in the facility and that the contribution of conduction heat transfer is negligible. While this work provides insights into the difference between ANSYS and COMSOL in modeling flow and heat transfer in a complex geometry, it does not ascertain which code is accurate. Experimental data are needed to validate the results from the CFD simulations.

### **Acknowledgment**

This work was funded by the Mission Supports and Test Services under Subcontract No. 287703.

### **References.**

- [1] U.S. DOE, 2008. "Technical Review Report for the Model 9975-96 Package Safety Analysis Report for Packaging (S-SARP-G-00003, Revision 0)." Packaging and Transportation Group Lawrence Livermore National Laboratory.
- [2] U.S. NRC, 2020. "10 CFR Part 71 - Packaging and Transportation of Radioactive Material," Nuclear Regulatory Commission.

- [3] Schreiber, J. 2007. “Nuclear Material Management for Nevada Test Site (NTS). Institution of Nuclear Materials Management.” Contract No. DE-AC52-06NA2594.
- [4] U.S. DOE, 2023. “10 CFR Part 830 – Safety Basis Requirements”, Department of Energy.
- [5] Kiflu, B. 2023. “NNS-DAF Enhanced Staging & Handling of Radioactive Material Packages.” PATRAM symposium.
- [6] Semprini, G., Jahanbin, A., Pulvirenti, B. and Guidorzi, P., 2019. “Evaluation of Thermal Comfort Inside an Office Equipped with a Fan Coil HVAC System: A CFD Approach.” *Future Cities and Environment*, 5(1), p.14.
- [7] Barbosa, B. P., Brum, N.C., 2018. “Validation and assessment of the CFD-0 module of CONTAM software for airborne contaminant transport simulation in laboratory and hospital applications” *Building and Environment*, 142, p. 139-152.
- [8] Flynt, A. “*ESP-491 HVAC CFD Modeling: Phase 2 CFD Report.*” Jacobs Engineering, Mar. 10, 2020.
- [9] Kaderaka, J. “A Scoping Study to Develop a Computational Fluid Dynamics Based Model to Predict Radiological Materials Packaging Temperatures within a Generic Staging Building.” M.S. Thesis, University of Nevada Reno.
- [10] COMSOL Multiphysics® v. 6.0. COMSOL AB, Stockholm, Sweden.
- [11] Ansys® Fluent, 2022 R1, Help System, ANSYS, Inc.



# Appendix A

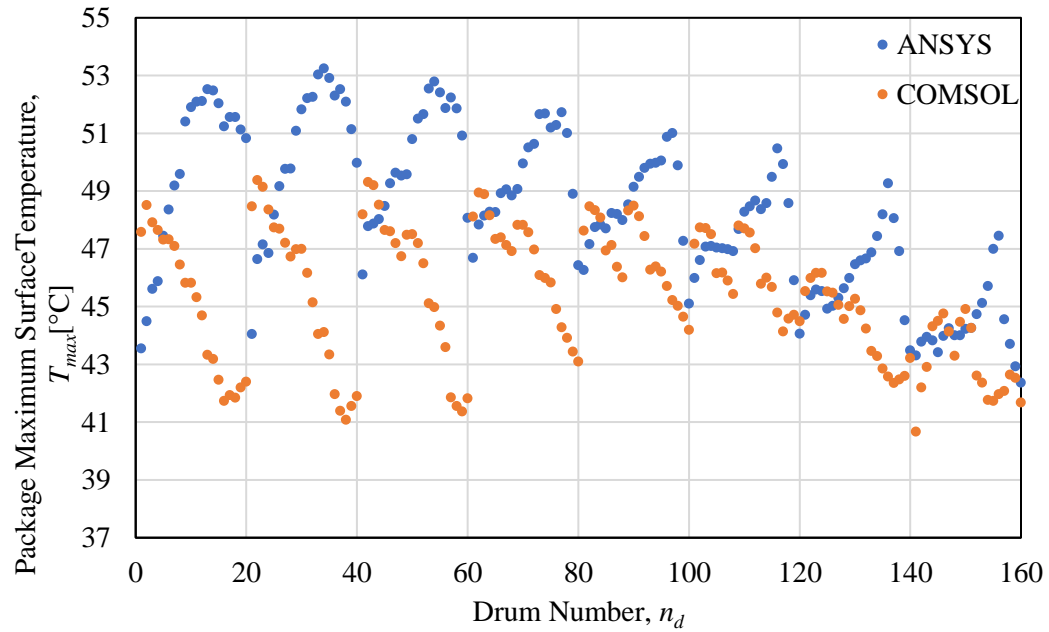


Figure A1: Individual Maximum Package Temperatures for COMSOL ( $C_{5M}$ ) and ANSYS ( $A_{22M}$ ) models in Row 1.

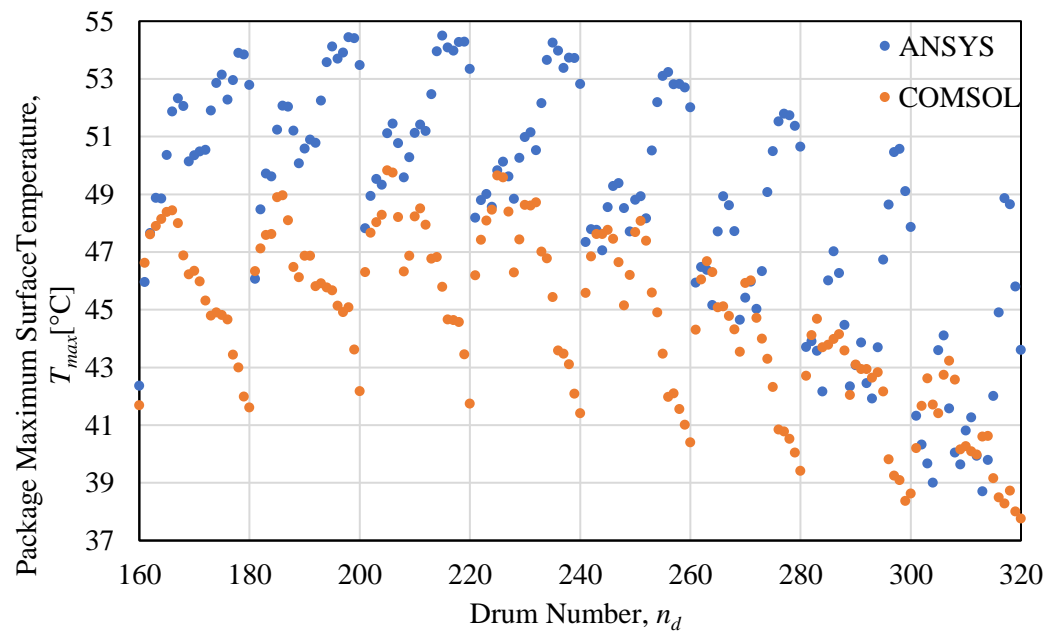


Figure A2: Individual Maximum Package Temperatures for COMSOL ( $C_{5M}$ ) and ANSYS ( $A_{22M}$ ) models in Row 2.

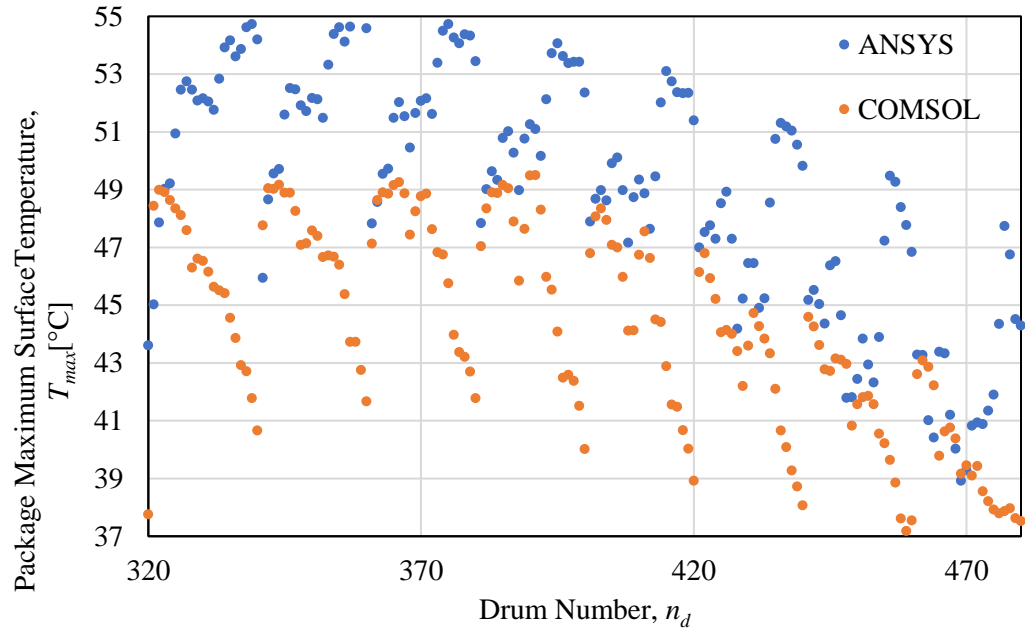


Figure A3: Individual Maximum Package Temperatures for COMSOL ( $C_{5M}$ ) and ANSYS ( $A_{22M}$ ) models in Row 3.

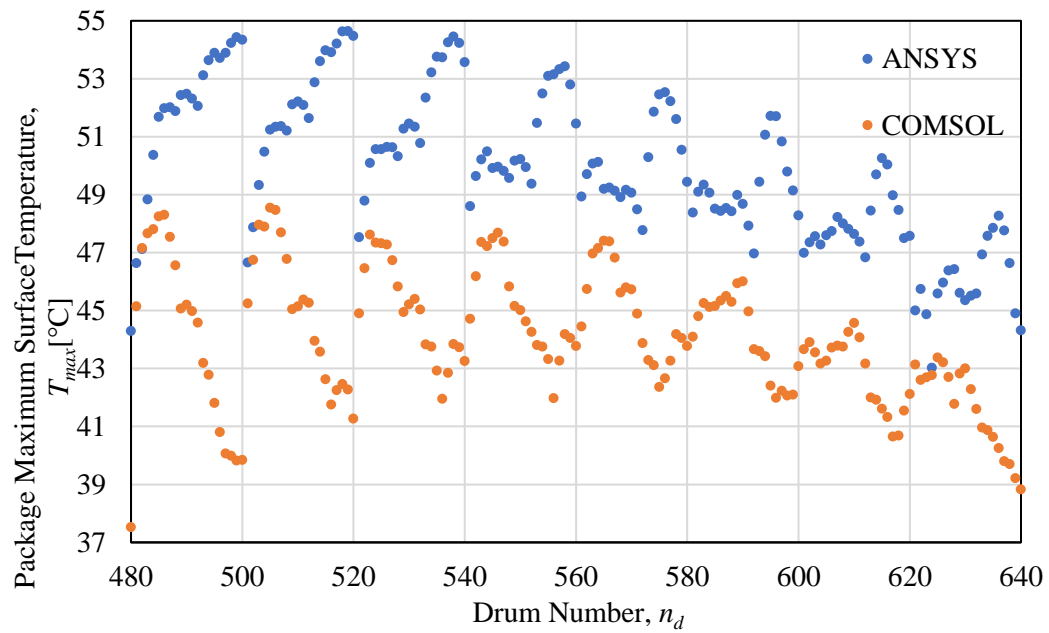
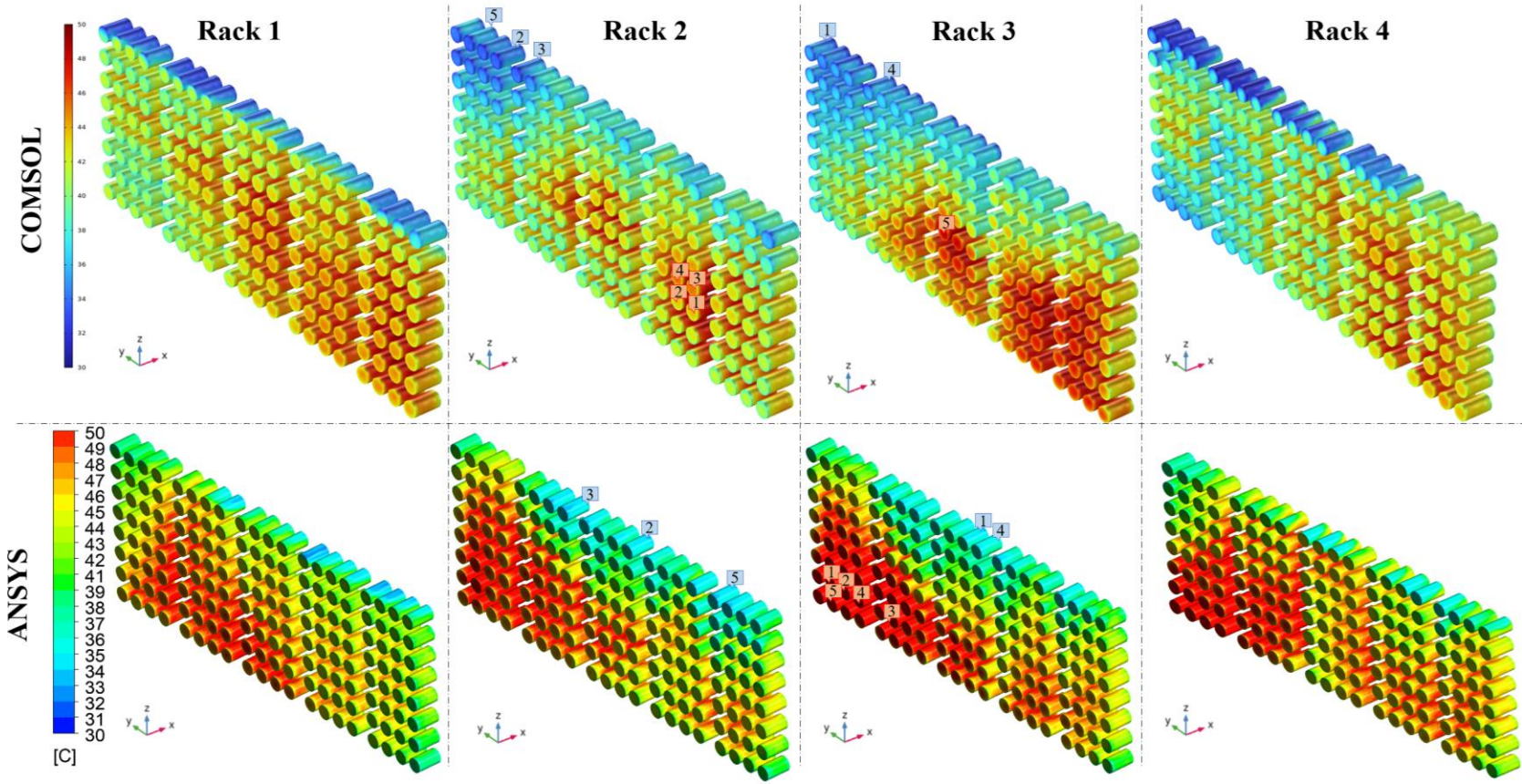


Figure A4: Individual Maximum Package Temperatures for COMSOL ( $C_{5M}$ ) and ANSYS ( $A_{22M}$ ) models in Row 4.



A5: Location of Coldest and Hottest Package Temperatures in  $C_{5M}$  and  $A_{22M}$